

An Experimental Study on Toughening Mechanisms of Fillers in Epoxy/ Silica Nanocomposites

M. Shariati¹, G.A. Farzi², A. Dadrasi^{3*}, M. Amiri² and R. Rashidi Meybodi^{4,5}

1. Department of Mechanics, Engineering Faculty, Ferdowsi University of Mashhad, Mashhad, I. R. Iran.
2. Department of Material and Polymer Engineering, Faculty of Engineering, Hakim Sabzevari University, Sabzevar, I. R. Iran.
3. Department of Mechanical Engineering, Shahrood University, Shahrood, I. R. Iran.
4. Department of Mechanical Engineering, Payame Noor University, Tehran, I. R. Iran.
5. Nano Structured Coatings Institute of Yazd Payame Noor University, Yazd, I. R. Iran.

(*) Corresponding author: ali.dadrasi@gmail.com

(Received: 14 March 2013 and Accepted: 10 Sep. 2015)

Abstract

In this paper, a systematic study on the effects of particle size and hybrid of two different size of silica nanoparticles on the toughening mechanisms of bisphenol-A epoxy was conducted. Nanosilica particles with mean diameter of 17 nm and 65 nm were blended into epoxy system. Probable synergy effects of these two nanoparticles on Young's modulus and yield strength have been investigated. Results showed that the addition of the silica nanoparticles and also increasing content of nanoparticles improved Young's modulus in all composites. In addition, the particle size did not show a considerable effect on the Young's modulus and the use of both types of particles in a composite showed negligible synergy effect. On the other hands, results revealed that the addition of these nanoparticles did not change the yield stress of composites significantly. The fracture surfaces of composites were studied by Scanning electron microscopy. It was revealed that in all three series of nanocomposites, crack deflection, crack forking and debonding were the most important mechanisms.

Keywords: Silica Nanoparticles, Crack deflection, Debonding, Toughening.

1. INTRODUCTION

The mechanical properties of an unmodified epoxy resin can be enhanced with the addition of different fillers [1-3]. Inorganic particles have drawn much attention for this purpose [4, 5].

Interestingly, the efficiency of inorganic particles is related to the type of toughening mechanisms that they can cause.

There are different toughening mechanisms propose explaining for toughness increasing of reinforced epoxy resin by particles in micron and nano size. Many researchers have observed that adding

nanoparticles to brittle materials increases the fracture energy [6-8].

The toughening mechanisms have been divided to two categories of in-plane process such as crack tip pinning or bowing [9] and crack path deflection [10], and out-plane process such as debonding and plastic void growth [11]. Some of these concepts are discussed in brief below.

1.1. Crack tip pinning or bowing

Crack tip pinning mechanism has been observed in nanocomposites reinforced by

particles in micron size [11-13] and also in nano size [15]. This draws parallels to the obstacle of the crack propagation by particles (dispersion hardening), e.g. [15], where the crack bows between particles, increasing its length.

As the energy of a crack is proportional to its length, additional energy input is required. Reducing the spacing between the particles and their size will increase the toughening effect [16].

Crack pinning mechanism has been explained by curve lines observed in fracture surface. Lange [10] has identified crack pinning phenomenon by curve lines of crack front in brittle materials such as glass and magnesium oxide.

But crack pinning phenomenon occurs when size of the particles are larger than crack-opening displacement.

So crack-opening displacement can be measured and compared with the particles size. Under plain strain condition, crack opening displacement, δ_{tc} , can be calculated by the following equation:

$$\delta_{tc} = \frac{K_{IC}^2}{E\sigma_y} (1 - \nu^2) = \frac{G_{IC}}{\sigma_y} \quad (1)$$

Where σ_y , E and ν are the yield stress, Young's modulus and Poisson's ratio of the matrix, respectively and k_{IC} and G_{IC} are fracture toughness and fracture energy of composite.

Green et al. [17] have shown that for crack pinning and bowing, it is necessary that particles sizes must be larger than plastic zone size at crack tip. According to Irwin's model under plain strain condition the assumption of liner elastic fracture mechanics (LEFM) and assuming that the plastic zone at crack tip is circular [18], radius of plastic zone can be expressed by:

$$r_y = \frac{1}{6\pi} \left(\frac{K_{IC}}{\sigma_y} \right)^2 \quad (2)$$

1.2. Crack path deflection

The toughening effect can occur by crack path deflection too. When crack reaches a rigid nanoparticle such as silica, it deflects and passes around it. This process leads to an increase in the fracture surface, attracts more energy and also causes the crack propagation happen under mixed mode I/II situation (See Figure 1[18]).

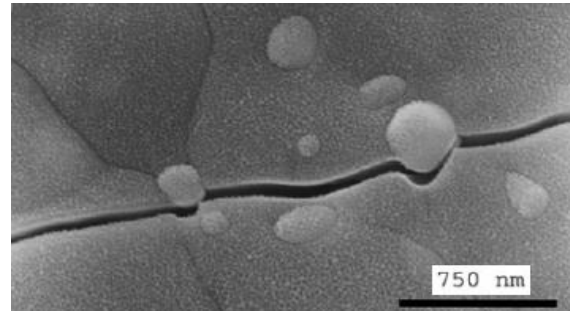


Figure1. Crack path deflection.

1.3. Deboning

In the study of fracture surface of some nanocomposites, researchers found that some of nanoparticles are deboned. This mechanism which is one of the out-plane process occurs with various shapes in debonding of different nanoparticles. Dittanet and Pearson [16] published pictures of fracture surface of epoxy composites containing 10 vol% of 170 nm, 74 nm, and 23 nm sized particles that showed random distribution of silica nanoparticles in epoxy matrix. They found the vacant spaces surrounding of some nanoparticles that proved these particles are deboned. Their images showed that only small portions of nanoparticles were deboned during fracture. Similar observations of debonding of silica nanoparticles have been reported by other researchers [19]. It's obvious that debonding depends on particles size [16, 19]. As nanoparticle size reduces, the number of deboned nanoparticles also decreases. The number of deboned particles decreasing might be due to the stronger bonds between the matrix and smaller nanoparticles.

It's expected that, particles size has a significant role in the type of toughening

mechanism. For example, the study of Zhang [14] showed that smaller nanoparticles improved composites properties by increasing the interface between particles and polymer matrix. Although Liang's [20] study about the effect of particles size, in the range of 20-80 nm, showed that this range did not any effect on the type of fracture or Young's modulus. Dittanet [16] reported that various size of silica nanoparticles did not change Young's modulus.

These differences show that the effect of particles size is not well understood especially in nanoscale, so the role of particles size on toughening mechanism need more study.

This study of literature shows various results on the effect of particles size on toughening mechanism of epoxy resin reinforced by silica nanoparticles. On the other hand the effect of using various diameter of silica nanoparticles for reinforcing epoxy resin matrix has not been studied (bimodal particle size systems), so this effect has been studied in this work.

2. DETAILS OF EXPERIMENT

2.1. Materials

The epoxy resin was standard diglycidyl ether of bis-phenol A (DGEBA) with an epoxy equivalent weight (EEW) of 189 g/mol, 'ML-504', supplied by Mokarrar, Iran. The spherical silica nanoparticles (SiO_2) with mean diameter of 17 and 65 nm and purity of more than 99.5% were provided by us-nano, USA. It is necessary to mentioned that particle range with medium diameter of 17 nm was between 15-20 nm and particle rang with medium diameter of 65 nm was between 60-70 nm. The curing agent, cycloaliphatic polyamine, HA-12, (Mokarrar, Iran.), was used nominally.

2.2. Composite preparation method

The neat epoxy resin has been reinforced by adding 1.5 to 6 wt% of silica nanoparticles. This epoxy has relatively low viscosity and

is suitable for using in sensitive molding systems without any defect in final model. Material formulations were prepared by mixing resin with certain weight fraction of nanoparticles for about two hours. These components were degassed, mixed for 10 minutes using a mechanical stirrer at 300 rpm and 50° C. Then polyamine hardener, HA-12, was added to the mixture. After 5 minutes mixing, the compound was poured into release-coated molds. Before testing, materials were cured at 160 °C for 6 h to remove any residual stress entered during the fabrication process.

For Samples coding, "NE" denotes neat epoxy and composites reinforced with 17 nm and 65 nm particle size are denoted by "S" and "L" letter, respectively and also bimodal particle size systems are denoted by both letters. The number behind these letters shows the weight fraction of silica nanoparticles.

2.3. Tension test

Uniaxial tensile tests were conducted in accordance with ASTM D638 standard. For this purpose, an Instron 8802 with 5 mm/min crosshead speed was used, shown in Figure 2. All samples were molded in a dog-bone form of dimensions of 3×19×185 mm. Tests were performed on at least four samples for each material composition under ambient temperature. The longitudinal strain was measured by a 50 mm gauge length and the Young's modulus, E, was calculated. 0.2 % offset strain was used for catching of yielding.

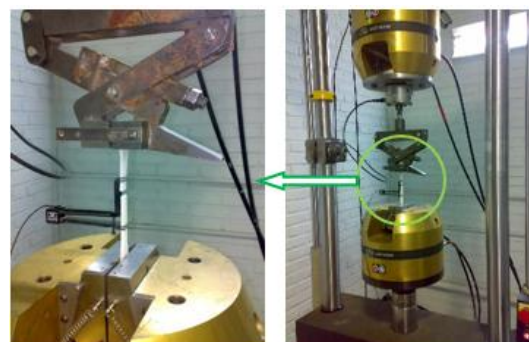


Figure 2. Tension test by Instron 8802 machine.

3. RESULTS AND DISCUSSION

3.1. Young's modulus and yield strength

Table 1 shows the amounts of Young's modulus and yield strength obtained from tensile test.

Obtained Young's modulus for neat epoxy resin is 1521 Mpa. The results of table 1 show that the Young's modulus clearly increases with the addition of nanosilica particles. Also, for all composites, the Young's modulus increases with increasing the weight fraction of silica nanoparticles but the effect of particles size on Young's modulus is not noticeable. This was confirmed by measuring the Specific surface area of both particle sizes. Similar observations of the effect of particles size have been reported in the literature [21, 22].

Maximum increase in Young's modulus for composites reinforced with a one type of particles ("S" series or "L" series) is in "6.0% S" composite and for composites reinforced with hybrid of both type of particles is in "3.0 % L- 3.0% S" composite. Table 1 also shows that in the same weight fraction of nanoparticles, Young modulus of composites reinforced with hybrid of both type of particles is a little more than composites reinforced with a one type of particles.

Another result from table 1 is that in both unimodal and bimodal particle size systems the yield strength is neither changed with the addition of silica nanoparticles, nor with nanoparticles content. This trend is in agreement with the literature [23, 24]. In order to understand the phenomenon, the interfacial strength between particle and polymer matrix should be considered. This interaction is particularly important for systems associated with nanoparticles, because they impart a large amount of surface area. When polymer materials are reinforced with rigid inorganic particles, a poor filler-matrix interfacial layer will be formed. In this case the filler cannot transfer the stress to the polymer matrix well [25]. On the other hands, the yield strength is not only affected by the interfacial strength

between particles and polymer matrix and properties of the matrix materials (e.g. ductile or brittle) and the shape of the fillers affect this parameter.

3.2. Study of microstructure

Table1. Young's modulus and yield strength of composite by different compound of reinforces.

Specimen Code	Total volume fraction (Vol %)	Young's modulus (Mpa)	Yield strength, σ_y , (Mpa)
NE	0	1521	20.3
1.5 % S	0.699	1547	19.6
3.0 % S	1.41	1589	19.9
4.5 % S	2.13	1605	19.2
6.0 % S	2.86	1712	19.7
1.5 % L	0.699	1535	20.1
3.0 % L	1.41	1572	19.5
4.5 % L	2.13	1591	20.4
6.0 % L	2.86	1684	20.2
1.5 % L- 1.5 % S	1.41	1565	19.8
1.5 % L- 3.0 % S	2.13	1653	20.3
1.5 % L- 4.5 % S	2.86	1723	19.1
3.0 % L- 3.0 % S	2.86	1735	20.5

Fracture surface of samples have been studied by scanning electron microscopy (Phenom pro X-811). All specimens were coated with a thin layer of gold with thickness of approximately 3-5 nm before analysis. An acceleration voltage of 20 kV was used. Figures 3 and 4 show SEM photographs of "6.0 % S" composite and "1.5 % L-4.5 % S" composite, respectively. It's obvious that in both composites, nanoparticles are uniformly dispersed in the epoxy matrix.

Two-dimensional view and topography of the fracture surfaces of neat epoxy and "6.0 % L" composite are shown in Figure 5 and 6, respectively. Figure 5 shows that the fracture surface of neat epoxy is relatively smooth and glassy and shows that no large-scale plastic deformation has occurred during fracture [25].

Also as shown in Figure 5, in the neat epoxy, crack surface transfers gently from one layer to another, the height of layers is

low and the height difference between these layers is not considerable. In addition, layers are fine and similar to each other, whereas in “6.0 % L” composite, the fracture surface is so layered, see Figure 6.

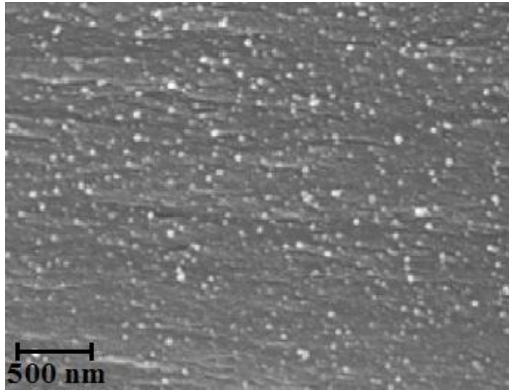


Figure3. SEM images of fracture surfaces of “6.0 % S” composite.

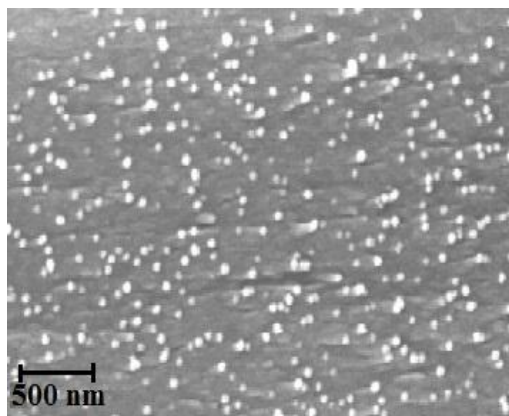


Figure4. SEM images of fracture surfaces of “1.5 % L-4.5 % S” composite.

This phenomenon is because of crack deflection mechanism. In the path of crack growth when the crack tip encounters with a nanoparticle, tilts and twists around it [25]. As a result, height difference of layers in fracture surface of nanocomposites is more than neat epoxy. Some of the layers are similar to the wing and are branched from the other layers. Such features are created by crack forking due to the extra energy associated with the fast crack growth. Forking repetition and the multi-planar nature of the surface are two ways for absorbing the extra energy in a very brittle material [26].

In some parts, the crack energy is not high enough to make a new surface and after a

little growth, it stops. It is indicated by white circle in Figure 6.a.

Crack deflection raises the surfaces roughness and makes crack path longer, increases the total fracture surface area and also grow locally under mixed-mode I/II [27]. For example, in depicted arbitrary green line on surface topography in Figures 6.a and 6.b, roughness difference between highest and lowest points is $21.81 \mu\text{m}$ and $128.56 \mu\text{m}$, respectively.

In more magnification, the effect of nanoparticles can be observed better. Figure 7 that shows the fracture surface of “6.0 % L” composite, indicates how nanoparticles cause crack front transfer from one layer to another.

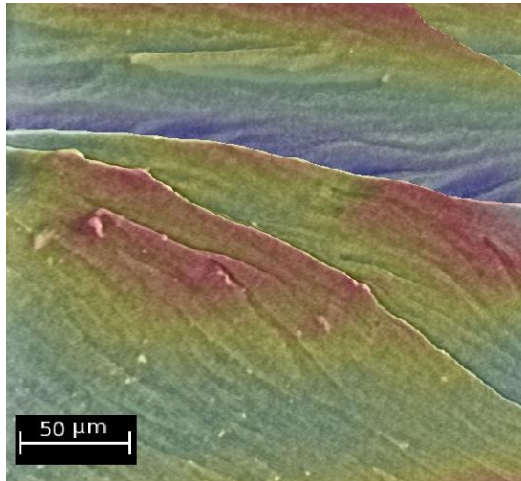
Figure 8 shows the fracture surfaces of “4.5 % L” composite that indicates another effective toughening mechanism is debonding of nanoparticles. White circles in this Figure show cavities around some of nanoparticle. These cavities prove some interactions between particles and matrix are deboned. These voids show that nanoparticles remained on the other fracture surface of sample or have fallen out of the surface completely during fracture.

The diameter of these voids is bigger than particle size. This is because of plastic void growth mechanism of the epoxy matrix, initiated by debonding of the nanoparticles. Based on the experimental studies [6, 19, 20], one of the major mechanisms for energy dissipating in epoxy-nanosilica composite is debonding of silica nanoparticles which enables the formation of plastic void growth in the matrix.

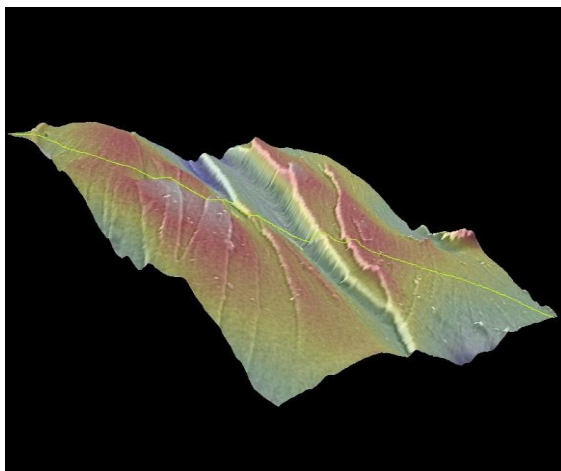
4. CONCLUSION

In this research the reinforcement effects of epoxy matrix with silica nanoparticles by two different size and various compounds were studied. The results showed that the Young’s modulus increase with adding silica nanoparticles in all composites and with increasing the content of particles too. It is observed that the particle size and use of two different size of nanoparticles in

bimodal systems didn't have considerable effect on Young's modulus. In both unimodal and bimodal particle size systems the yield strength didn't change with the addition of silica nanoparticles. The study of fracture surface of specimens showed that in all series of specimens, crack path deflection, crack forking and nanoparticles debonding are the most important mechanism.



a) Two-dimensional view

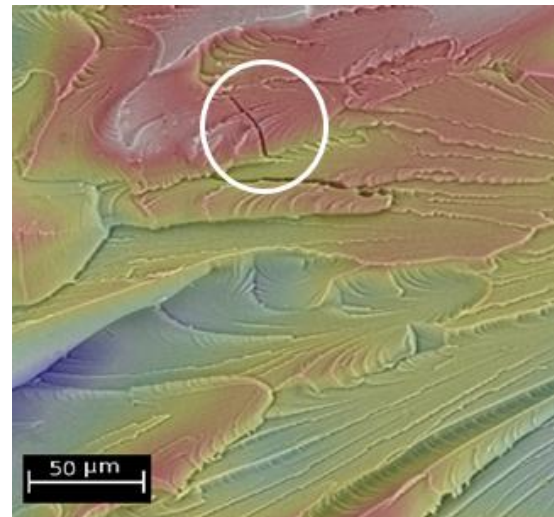


b) Surface topography

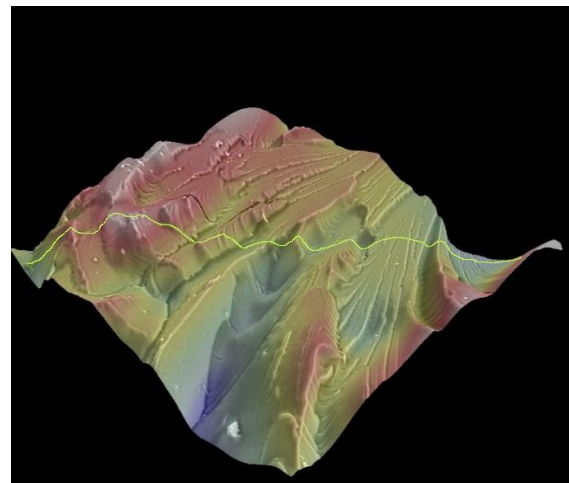
Figure5. SEM images of fracture surfaces of neat epoxy

ACKNOWLEDGMENT

I'd like to thank all members of "Nano Structured Coatings Institute of Yazd Payame Noor University" for their valuable help.



a) Two-dimensional view



b) Surface topography

Figure6. SEM images of fracture surfaces of "6.0 % L" composite.

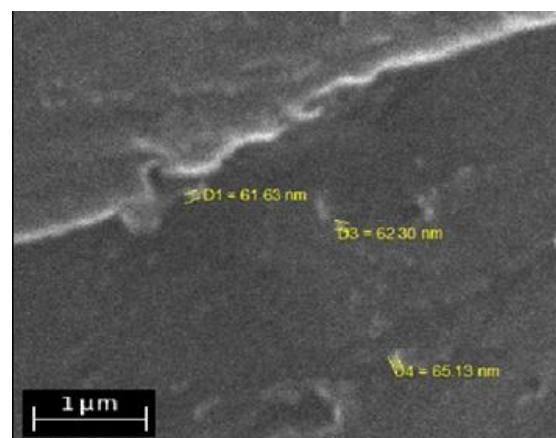


Figure7. SEM images of fracture surfaces of "6.0 % L" composite.

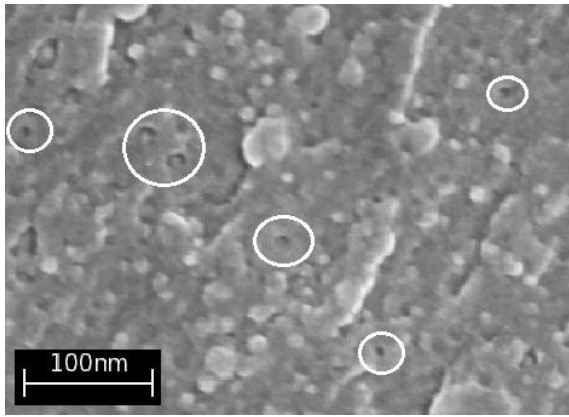


Figure 8. SEM image of fracture surfaces of "4.5 % L" composite.

REFERENCES

1. Q.H. Qin: Tough. Mechanisms Compos. Mat., Vol. 15, (2015), pp. 1-32.
2. J. Li and Sh. Chen: Mater. Lett., Vol. 121, (2014), pp. 174-176.
3. Y. Lin, Y. Lei, H. Fu and J. Lin: Mater. Des., Vol. 80, (2015), pp. 82-88.
4. M. Quaresimin, M. Salviato and M. Zappalorto: Tough. Mechanisms Compos. Mat., Vol. 25, (2015), pp. 113-133.
5. H. Liang, X. Yao, H. Zhang, X. Liu and Z. Huang: Ceram. Int., Vol. 40, (2014), pp. 10699-10704.
6. T. H. Hsieh, A. J. Kinloch, K. Masania, A.C. Taylor and S. Springer: Polym., Vol. 51, (2010), pp.6284-6294.
7. R. Hashemi- Nasab and S. M. Mirabedini: Prog. Org. Coat., Vol. 76, (2013), pp.1016-1023.
8. R. Kitey and H. V. Tippur: Acta Mater., Vol. 53, (2005), pp. 1153-1165.
9. F. F. Lange and J. A. Ceram. Soc., Vol. 54, (1971), pp.604-620.
10. F.F. Lange: Philos. Mag., Vol. 22, (1970), pp. 983-92.
11. A. J. Kinloch, D. L. Maxwell, R. J. Young: J Mater Sci, Vol. 20, pp. 4169-84.
12. J. Spanoudakis, R. J. Young: J Mater Sci., Vol. 19, (1984), pp. 473-86.
13. F. F. Lange, K. C. Radford, J Mater Sci, Vol. 6, (1971), pp. 1197-203.
14. H. Zhang, Z. Zhang, K. Friedrich, C. Eger: Acta Mater., Vol. 54, (2006), pp.1833-42.
15. R.M. Caddell: Deformation and fracture of solids, (1980), Englewood Cliffs, New Jersey: Prentice-Hall.
16. P. Dittanet, R.A. Pearson: Polym., Vol. 53, (2012), pp. 1890-1905.
17. D.J. Green, P. S. Nicholson, J.D. Embury: J Mater Sci, Vol. 14, (1979), pp.1657-61.
18. G.R. Irwin: Fracture in Handbook of physics, (1958), Vol. 6, Springer-Verlage, Heidelberg, pp. 551-590.
19. B. B. Johnsen, A. J. Kinloch, R. D. Mohammed, A. C. Taylor and S. Springer: Polym, Vol. 48, (2007), pp.530-541.
20. Y.L. Liang and R.A. Pearson: Polym, Vol. 50, (2009), pp. 4895-905.
21. J. T. Choi, D. H. Kim, K. S. Ryu, H. Lee, H. M. Jeong, C. M. Shin, J. H. Kim and B. K. Kim: Macromol. Res., Vol. 19, (2011), pp.809-814.
22. A. Vinayak, P. Dhumale, V. Shah, B. Rishi, B. Sharma and T. Katsuaki: Bull. Mater. Sci, Vol. 35, (2012), pp. 143-149.
23. K.J. Pascoe: An introduction to the properties of engineering materials, (1978), 3rd ed. London: Van Nostrand Reinhold.
24. P. Dittanet, R. A. Pearson: Polym., Vol. 54, (2013), pp. 1832-1845.
25. A. J. Kinloch, A. C. Taylor: J. Mat. Sci, Vol. 37, (2002), pp. 433-60.
26. E. H. Andrews: Fracture in polymers, (1968), 1st ed. Edinburgh: Oliver & Boyd.
27. K.T. Faber, A.G. Evans: Acta Metall., Vol. 31, (1983), pp.565-76.